Electronic Supplementary Information

for

Cu and Ni dual-doped ZnO nanostructures templated by cellulose nanofibrils with boosted visible light photocatalytic degradation of wastewater pollutants

Contents

Experimental

Catalyst characterization

Fourier transform infrared spectroscopy (FT-IR) was performed on a Nicolet 6700 by using the KBr pellet technique with a resolution of 2 cm^{-1} from 500 to 4000 cm^{-1} and consisted of 32 scans at room temperature. The BET surface area of the catalyst was measured by the adsorption of N_2 at -196 °C (Micromeritics, ASAP2460, USA). The X-ray diffraction (XRD) patterns were obtained using an X-ray diffractometer (Bruker, D8 advance, Germany) operated with Cu-Kα radiation at 40 kV and 40 mA with a scanning rate of 2 degree·min^{-1}. The crystallite size (D) was calculated using the Debye-Scherer formula (1) and the microstrain (ε) using the following equations (2), as follows:[1]

$$D = \frac{k\lambda}{\beta \cos\theta} \quad (1)$$

$$\varepsilon = \frac{\beta}{4\tan\theta} \quad (2)$$

where k is the constant (k = 0.9), θ is the Bragg diffraction angle, λ is the X-ray source wavelength (λ = 1.54056 Å), and β is the full width at half maximum (FWHM). X-Ray photoelectron spectroscopy (XPS) was carried out at 15 kV and 5 mA (Shimadzu, AXIS Ultra DLD, Japan), with the binding energies calibrated at 284.6 eV from C 1s of the adventitious carbon. Scanning electron microscopy (Hitachi, SU8010, Japan) for the sample morphology was conducted at 10 kV and 10 mA. The elemental distribution of the ZnO@CNF nanocomposites was studied using energy dispersive spectrometry (EDS). Additionally, the optical absorption spectra of the specimens were corroborated using a UV-Vis spectrum analyzer (PerkinElmer, Lambda 650S, USA) equipped with an integrated sphere ($BaSO_4$ was used as the reference). Photoluminescence (PL) spectra were obtained at room temperature on a fluorescence lifetime spectrophotometer (Horiba, Quanta Master 8000, Canada) with an excitation wavelength of 370 nm. Thermogravimetric analysis (TGA) was conducted under N_2 atmosphere with a programmed heating rate of 10 °C/min from 50 to 800 °C (PerkinElmer, STA8000, USA).

The photocurrent response measurements were conducted on a CHI760E electrochemical workstation in a three-electrode system. The catalyst powder (10 mg) was ultrasonicated in a 5% ethanol solution to obtain a slurry. After that, 150 µL slurry was dispersed onto Indium tin oxide (ITO) glass with drying treatment at room temperature. The electrodes were immersed in 0.5 mol L^{-1} sodium sulfate aqueous solution. The counter electrode and reference electrode were the platinum plate and silver-silver chloride electrodes, respectively. For electrochemical impedance spectroscopy (EIS) experiments, the perturbation signal was 5 mV, and the frequency ranged from 0.1-100 kHz. The working electrode was irradiated with a 300 W xenon lamp during the measurement.

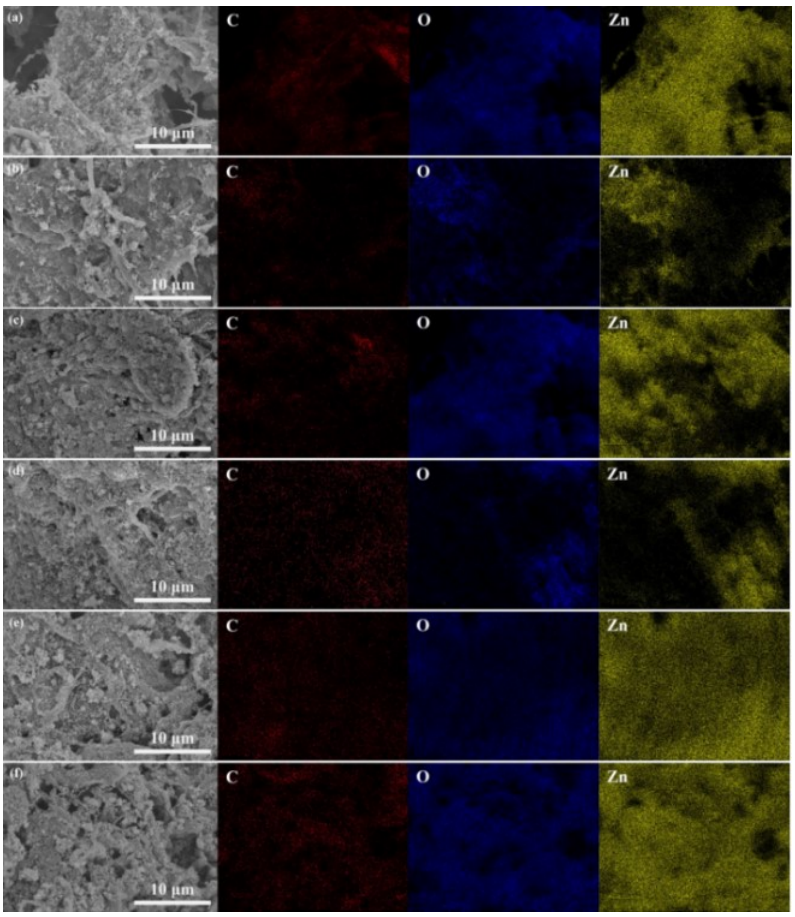

Fig. S1 EDS mapping of (a) $ZnO_{0.2}$@CNF, (b) $ZnO_{0.3}$@CNF, (c) $ZnO_{0.4}$@CNF, (d) $ZnO_{0.5}$@CNF, (e) $ZnO_{0.6}$@CNF and (f) $ZnO_{0.7}$@CNF.

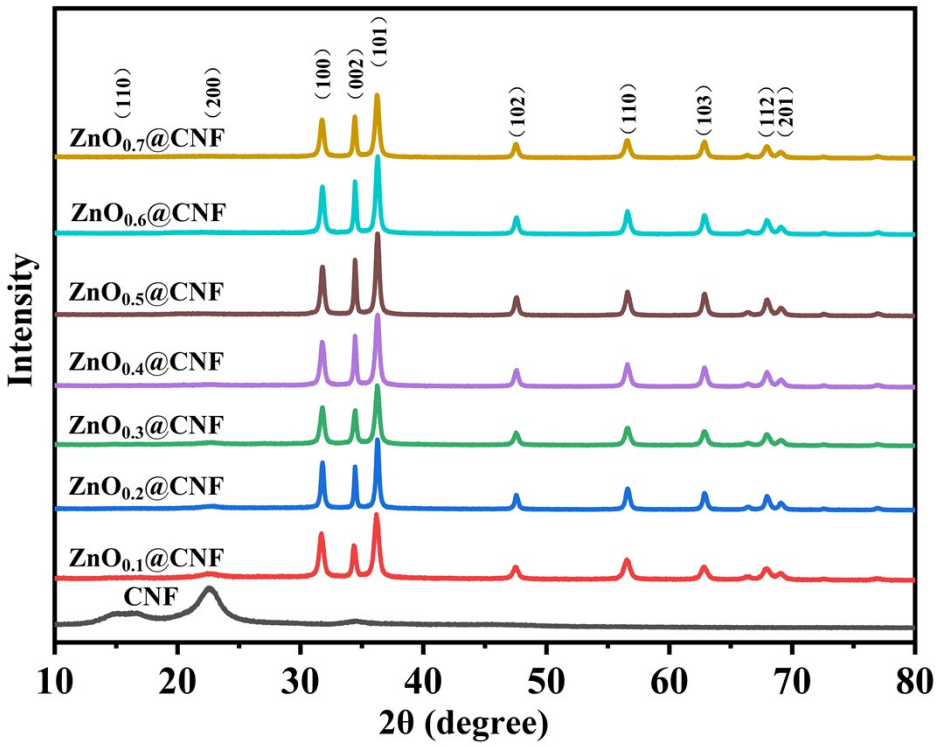

Fig. S2 XRD patterns of $ZnO_{0.2}$@CNF, $ZnO_{0.3}$@CNF, $ZnO_{0.4}$@CNF, $ZnO_{0.5}$@CNF, $ZnO_{0.6}$@CNF and $ZnO_{0.7}$@CNF.

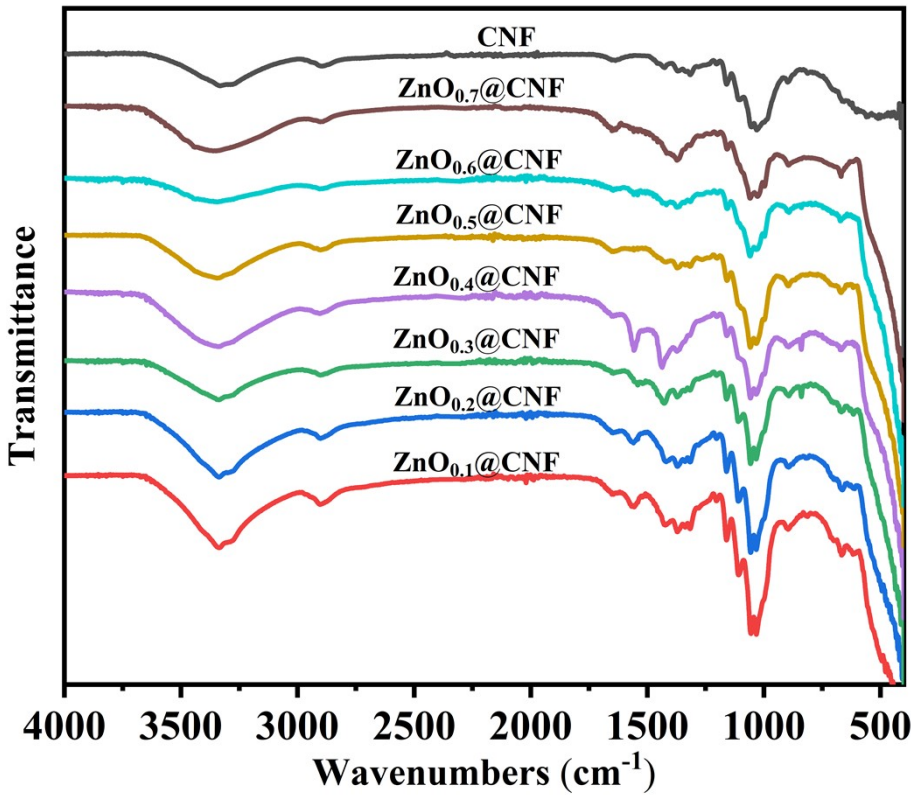

Fig. S3 FT-IR spectra of $ZnO_{0.2}$@CNF, $ZnO_{0.3}$@CNF, $ZnO_{0.4}$@CNF, $ZnO_{0.5}$@CNF, $ZnO_{0.6}$@CNF and $ZnO_{0.7}$@CNF.

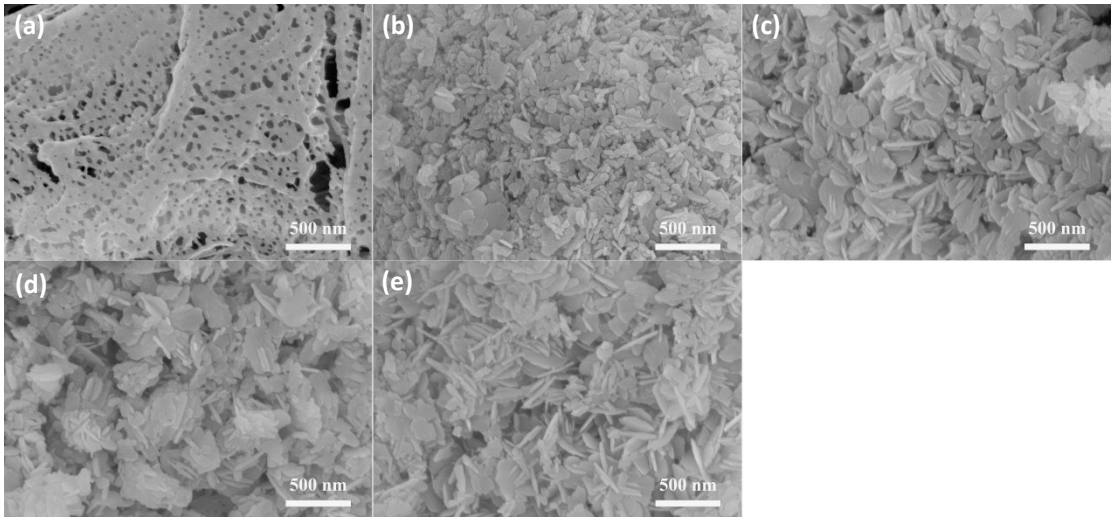

Fig. S4 SEM images of CNF, $ZnO_{0.6}$@CNF, Cu-$ZnO_{0.6}$@CNF, Ni-$ZnO_{0.6}$@CNF and Cu/Ni-$ZnO_{0.6}$@CNF.

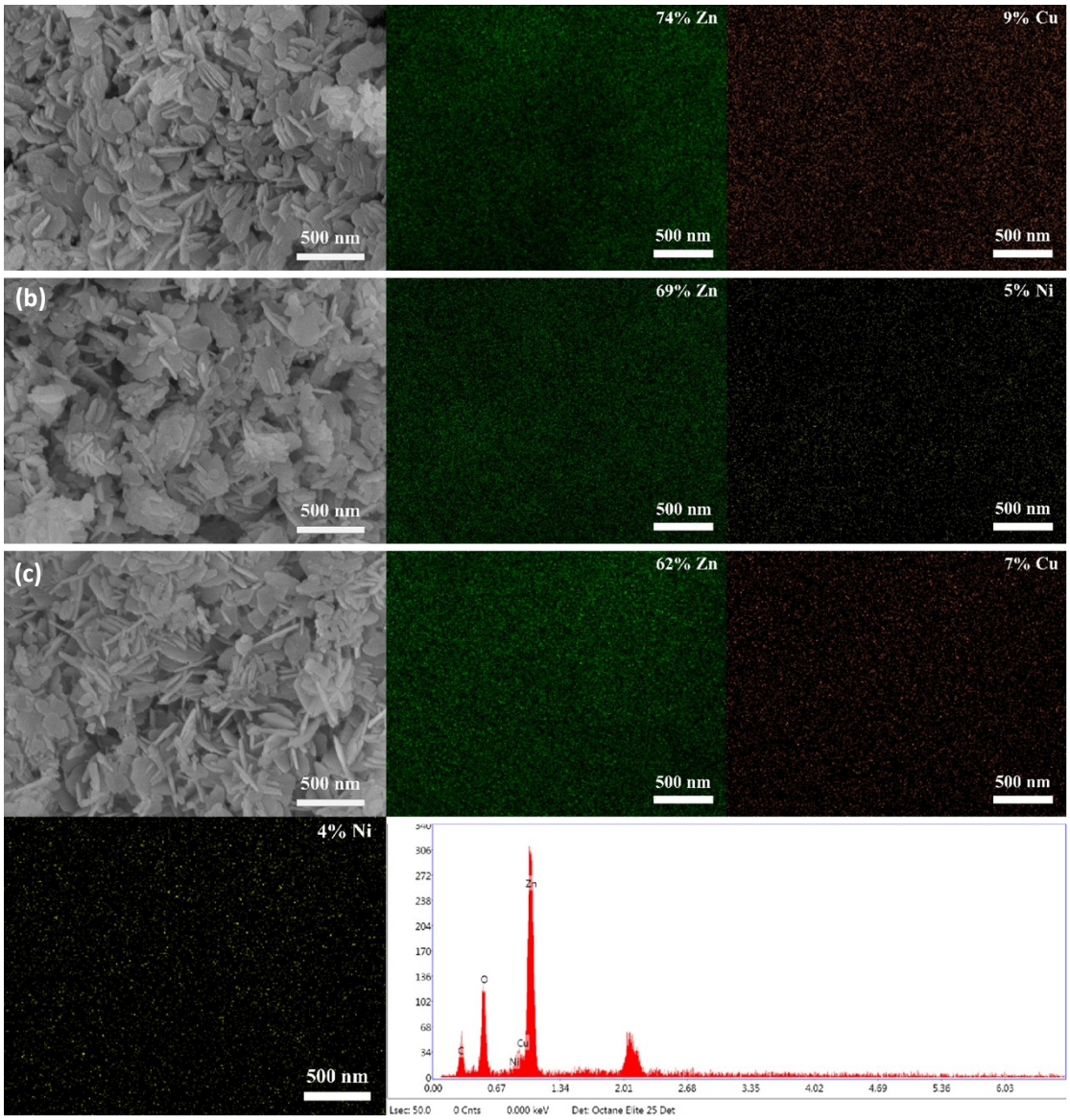

Fig. S5 EDS mapping of $ZnO_{0.6}$@CNF, Cu-$ZnO_{0.6}$@CNF, Ni-$ZnO_{0.6}$@CNF and Cu/Ni-$ZnO_{0.6}$@CNF.

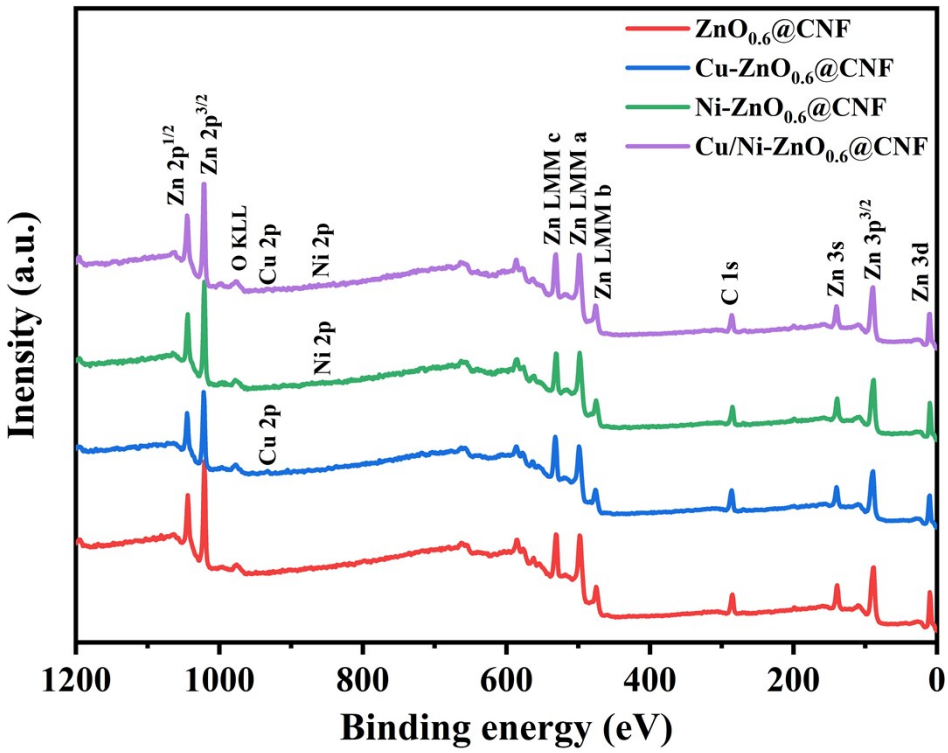

Fig. S6 Full survey XPS spectra of pristine and doped $ZnO_{0.6}$@CNF nanocomposites.

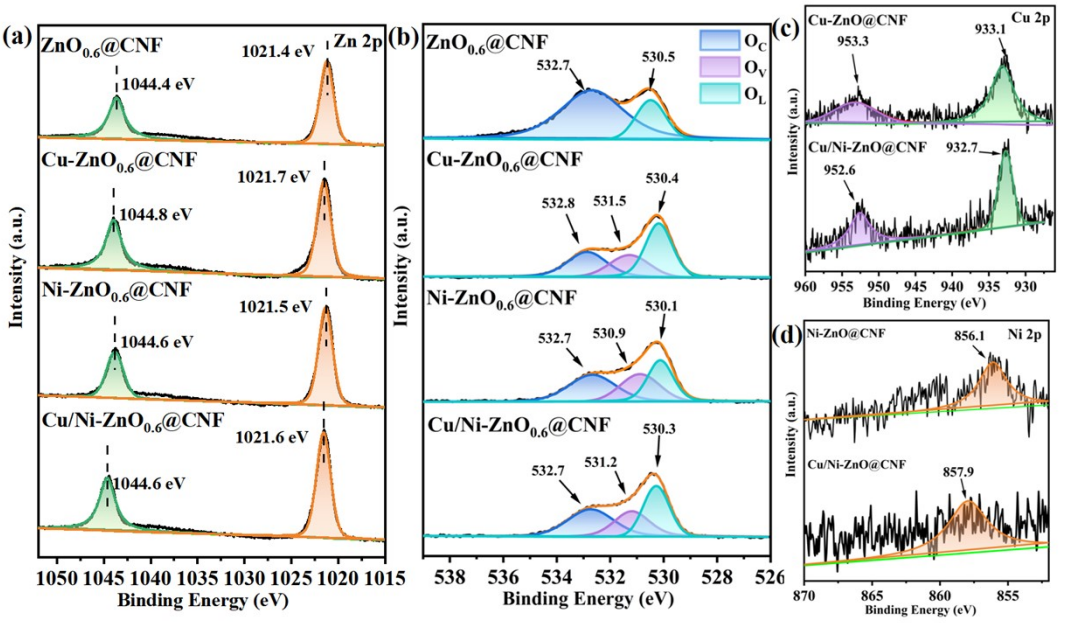

Fig. S7 XPS spectra of pristine and doped $ZnO_{0.6}$@CNF nanocomposites: (a) Zn 2p, (b) O 1s, (c) Cu 2p and (d) Ni 2p.

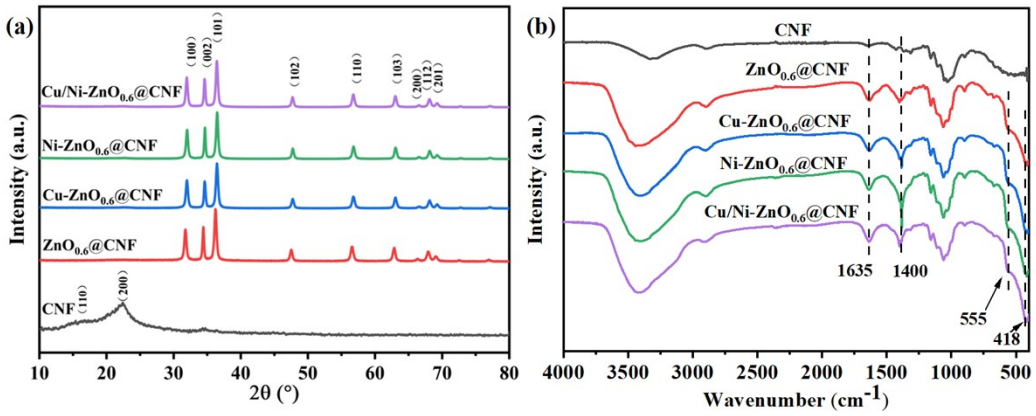

Fig. S8 (a) XRD patterns and (b) FTIR spectra of CNF, $ZnO_{0.6}$@CNF, Cu-$ZnO_{0.6}$@CNF, Ni-$ZnO_{0.6}$@CNF and Cu/Ni-$ZnO_{0.6}$@CNF.

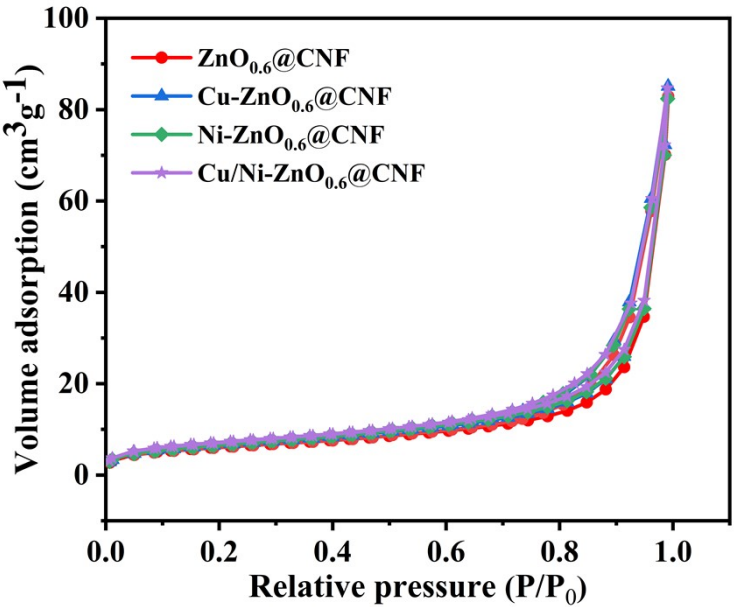

Fig. S9 BET curves of pristine and doped $ZnO_{0.6}$@CNF nanocomposites.

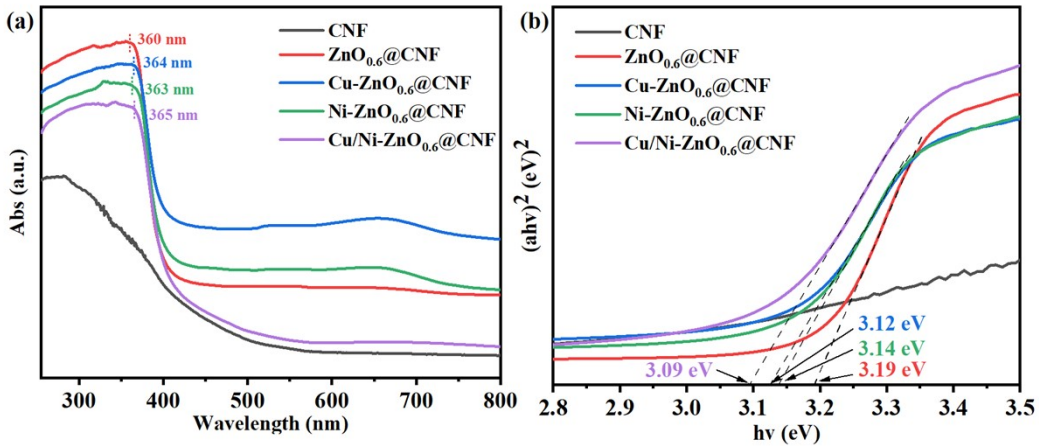

Fig. S10 (a) the UV-vis diffuse reflectance spectra and (b) bad gap energy of CNF, $ZnO_{0.6}$@CNF, Cu-$ZnO_{0.6}$@CNF, Ni-$ZnO_{0.6}$@CNF and Cu/Ni-$ZnO_{0.6}$@CNF.

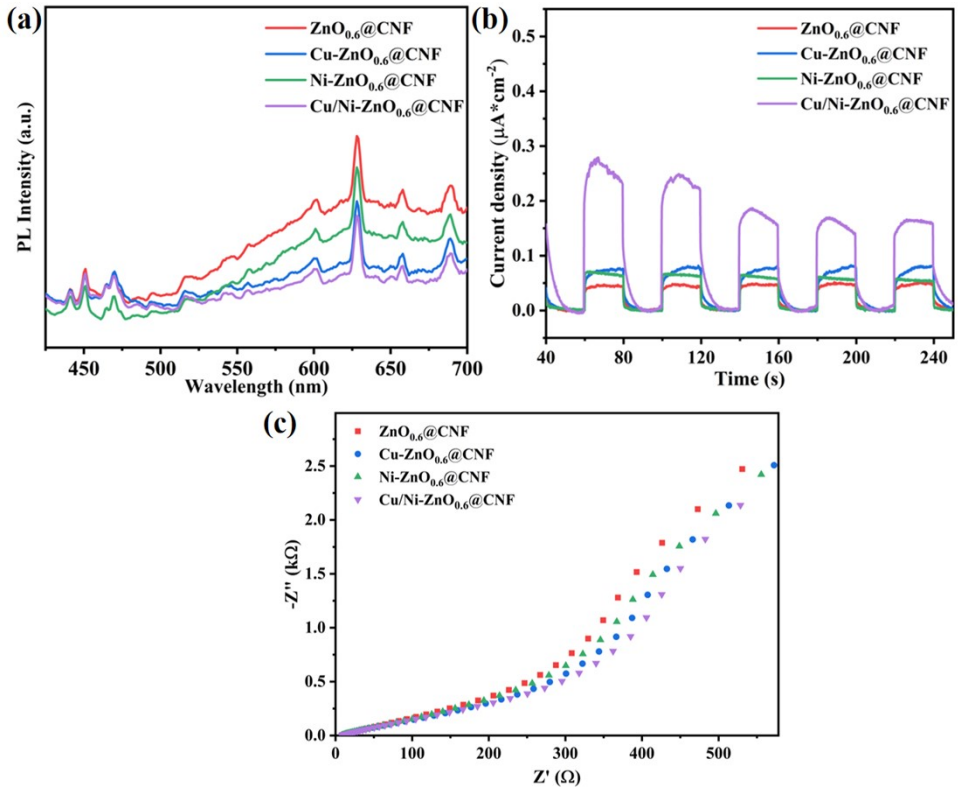

Fig. S11 (a) PL spectra, (b) photocurrent response curve and (c) EIS of pristine and doped $ZnO_{0.6}$@CNF nanocomposites.

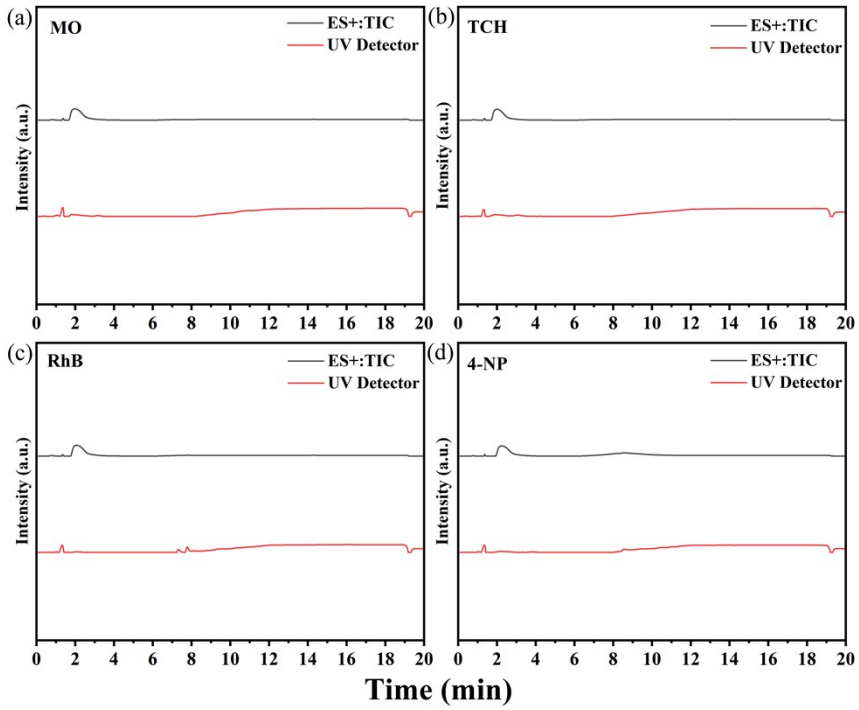

Fig. S12 LC-MS results of visible light photocatalytic degradation of wastewater pollutants

Tab. S1 Structural parameters of pristine and doped $ZnO_{0.6}$@CNF nanocomposites.

Samples	(h,k,l)	2θ /deg	d	β /deg	D /nm	ε /10^{-3}
$ZnO_{0.6}$@CNF	100	31.8	2.82	0.38	20.4	1.14
	002	34.4	2.60	0.25	31.0	0.76
	101	36.2	2.48	0.37	20.2	1.16
Cu-$ZnO_{0.6}$@CNF	100	32.0	2.80	0.40	19.0	1.22
	002	34.6	2.59	0.29	26.5	0.88
	101	36.5	2.46	0.39	19.3	1.22
Ni-$ZnO_{0.6}$@CNF	100	32.0	2.80	0.39	19.7	1.18
	002	34.3	2.46	0.28	27.4	0.86
	101	36.5	2.46	0.38	20.0	1.18
Cu/Ni-$ZnO_{0.6}$@CNF	100	31.9	2.80	0.38	19.7	1.18
	002	34.6	2.59	0.28	27.4	0.86
	101	36.5	2.46	0.38	20.0	1.18

Notes and references

1. A. Arfaoui, A. Mhamdi, B. Khalfallah, S. Belgacem and M. Amlouk, *Appl. Phys. A*, 2019, **125**, 517.